



Biologically active constituents from the fruiting body of *Taiwanofungus camphoratus*

Li-Shian Shi^{a,†}, Chih-Hua Chao^{b,†}, De-Yang Shen^b, Hsiu-Hui Chan^{b,†}, Chou-Hsiung Chen^b, Yu-Ren Liao^b, Shwu-Jen Wu^c, Yann-Lii Leu^d, Yuh-Chiang Shen^e, Yao-Haur Kuo^e, E-Jian Lee^f, Keduo Qian^h, Tian-Shung Wu^{b,g,*}, Kuo-Hsiung Lee^{h,g,*}

^a Department of Biotechnology, National Formosa University, Yunlin 632, Taiwan

^b Department of Chemistry, National Cheng Kung University, Tainan 701, Taiwan

^c Department of Medical Technology, Chung Hua University of Medical Technology, Tainan 717, Taiwan

^d Natural Products Laboratory, Graduate Institute of Natural Products, Chang Gung University, Kweishan, Taoyuan 333, Taiwan

^e National Research Institute of Chinese Medicine, Taipei 112, Taiwan

^f Department of Surgery, National Cheng Kung University Medical Center and Medical School, Tainan 701, Taiwan

^g Chinese Medicine Research and Development Center and Department of Pharmacy, China Medical University and Hospital, Taichung, Taiwan

^h Natural Products Research Laboratories, UNC Eshelman School of Pharmacy, University of North Carolina, Chapel Hill, NC 27599-7568, USA

ARTICLE INFO

Article history:

Received 5 August 2010

Revised 11 October 2010

Accepted 13 October 2010

Available online 20 October 2010

Keywords:

Taiwanofungus camphoratus

Fruiting bodies

Anti-inflammatory

NOX

ROS

Cytotoxicity

ABSTRACT

Five new benzenoids, benzocamphorins A–E (**1–5**), and 10 recently isolated triterpenoids, camphoratsins A–J (**16–25**), together with 23 known compounds including seven benzenoids (**6–12**), three lignans (**13–15**), and 13 triterpenoids (**26–38**) were isolated from the fruiting body of *Taiwanofungus camphoratus*. Their structures were established by spectroscopic analysis. Selected compounds were examined for cytotoxic and anti-inflammatory activities. Compounds **9** and **21** showed moderate cytotoxicity against MCF-7 and Hep2 cell lines with ED₅₀ values of 3.4 and 3.0 µg/mL, respectively. Compounds **21**, **25**, **26**, **29–31**, **33**, and **36** demonstrated potent anti-inflammatory activity by inhibiting lipopolysaccharide (LPS)-induced nitric oxide (NO) production with IC₅₀ values of 2.5, 1.6, 3.6, 0.6, 4.1, 4.2, 2.5, and 1.5 µM, respectively, which were better than those of the nonspecific nitric oxide synthase (NOS) inhibitor *N*-nitro-L-arginine methyl ester (L-NAME) (IC₅₀: 25.8 µM). These results may substantiate the use of *T. camphoratus* in traditional Chinese medicine (TCM) for the treatment of inflammation and cancer-related diseases. The newly discovered compounds deserve further development as anti-inflammatory candidates.

© 2010 Elsevier Ltd. All rights reserved.

1. Introduction

Niu-chang-chih also named *Taiwanofungus camphoratus* (synonym: *Ganoderma camphoratum*, *Antrodia cinnamomea*, *Antrodia camphorata*) (Polyporaceae, Aphyllophorales) is a rare and precious medical fungus in Taiwan.¹ The fruiting bodies of *Niu-chang-chih* have been used as a Chinese folk medicine for the treatment of liver diseases, food and drug intoxication, diarrhea, abdominal pain, hypertension, itchy skin and tumorigenic diseases in Taiwan.^{2,3} *Niu-chang-chih* has thus received huge attention by the

public. Previous studies have revealed that *Niu-chang-chih* exerts several biological activities, such as hepatoprotective effects, anti-hepatitis B virus effects, anticancer activity, antioxidant properties, and anti-inflammatory activities.^{4,5} Our ongoing study on the chemical constituents of an ethanol extract of the fruiting body of *T. camphoratus* has now led to the isolation of five new benzenoids, benzocamphorins A–E (**1–5**) (Fig. 1), 10 recently isolated triterpenoids, camphoratsins A–J (**16–25**) (Fig. 2), together with 23 known compounds including seven benzenoids (**6–12**) (Fig. 3), three lignans (**13–15**) (Fig. 4), and 13 triterpenoids (**26–38**) (Fig. 5).

Inflammation, which is related to morbidity and mortality of many diseases, is part of the complex biological response of vascular tissues to harmful stimuli, and is the host response to infection or injury, which involves the recruitment of leukocytes and the release of inflammatory mediators, including nitric oxide (NO). NO is the metabolic by-product of the conversion of L-arginine to L-citrulline by a class of enzymes termed NO synthases (NOS). Numerous cytokines can induce the transcription of inducible NO synthase

* Corresponding authors. Address: Department of Chemistry, National Cheng Kung University, Tainan, Taiwan (T.-S.W.); Natural Products Research Laboratories, UNC Eshelman School of Pharmacy, University of North Carolina, Chapel Hill, NC 27599-7568, USA. Tel.: +1 919 962 0066; fax: +1 919 966 3893 (K.-H.L.).

E-mail addresses: tswu@mail.ncku.edu.tw (T.-S. Wu), khlee@unc.edu (K.-H. Lee).

† These authors provided equal contributions to this work.

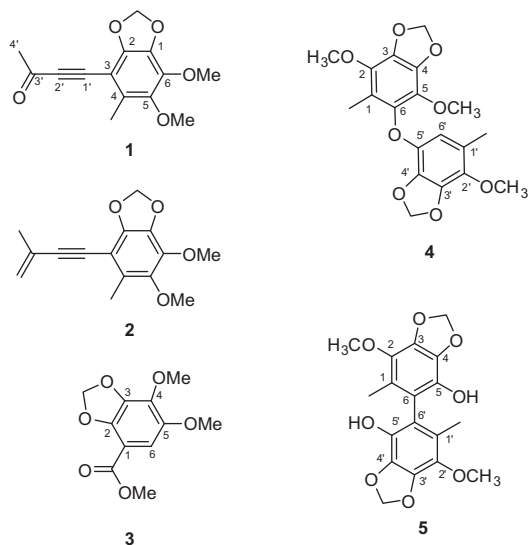


Figure 1. Structures of compounds 1–5.

(iNOS) in leukocytes, fibroblasts, and other cell types, accounting for enhanced levels of NO. Although NO is a microbicide and may have important roles in tissue adapting to inflammatory states, overproduction of NO may exacerbate tissue injury in both acute and chronic inflammatory conditions. In experimental models of acute inflammation, inhibition of iNOS can have a dose-dependent protective effect, suggesting that NO promotes edema and vascular permeability. NO also has a detrimental effect in chronic models of arthritis, whereas protection is seen with iNOS inhibitors. Glucocorticoids, which are often used in the treatment of inflammation, are able to inhibit the expression of iNOS. Therefore, the compounds isolated from *T. camphoratus* were tested for anti-inflammatory activity based on inhibition of NO production. In this paper, we report the structural determination of the new compounds from *T. camphoratus*, as well as evaluation of the cytotoxicity and anti-inflammatory activity of the isolates.

2. Chemistry: extraction and isolation

The wild fruiting bodies of *T. camphoratus*, growing in Ping-Tung Hsien, Taiwan, were purchased from the Kaohsiung

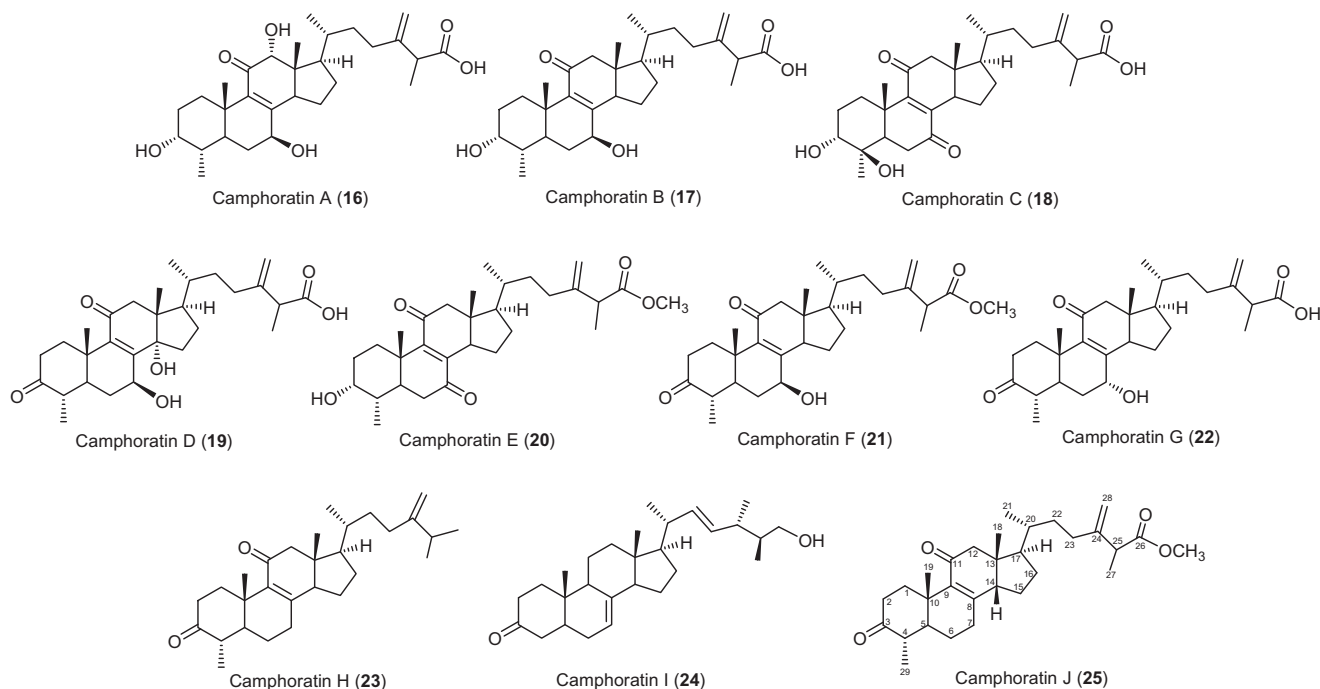


Figure 2. Structures of compounds 16–25.

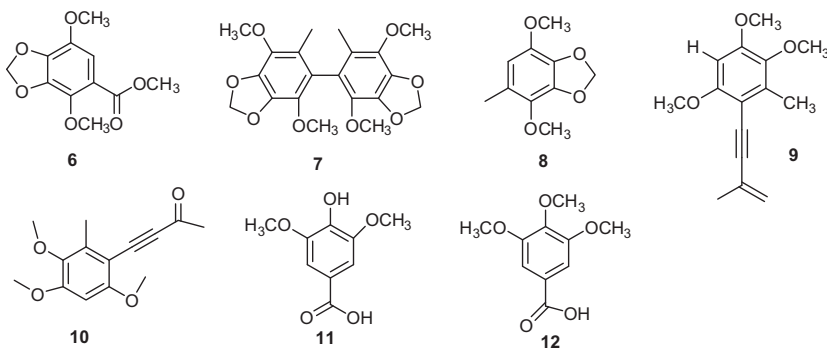


Figure 3. Structures of compounds 6–12.

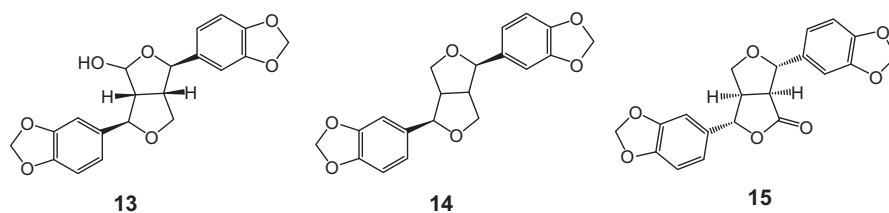


Figure 4. Structures of compounds 13–15.

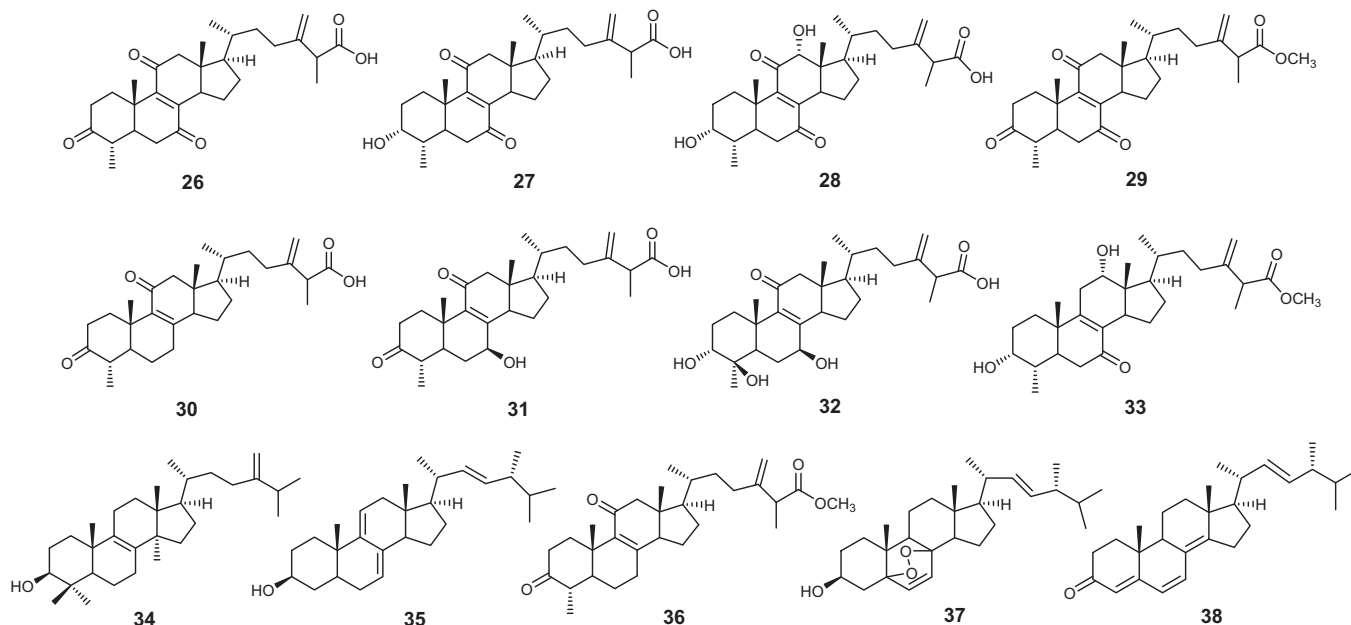


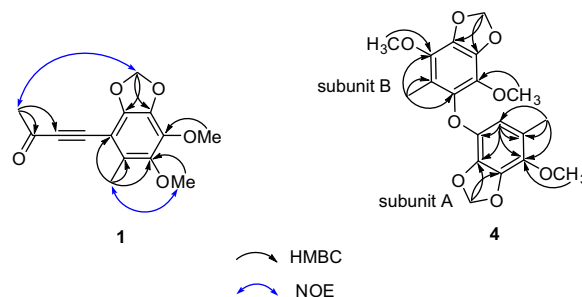
Figure 5. Structures of compounds 26–38.

Society for Wildlife and Nature in June 2003. The fungus was identified by Dr. Tun-Tschu Chang. A voucher specimen (TSWu 2003005) was deposited in the Department of Chemistry, National Cheng Kung University, Tainan, Taiwan.

The fresh fruiting body of *T. camphoratus* (1.0 kg) was extracted with EtOH (4×10 L) under reflux. The EtOH extract was concentrated to afford a brown syrup (161 g) and then partitioned between MeOH and H₂O (1:1) and *n*-hexane. The water layer was filtered to obtain a filtrate and a water-insoluble portion. The filtrate (55.5 g) was subjected to column chromatography on Diaion HP-20 (10 \times 60 cm) using increasing concentrations of MeOH in H₂O as the eluent to obtain 10 fractions (ACEW 1–10). Compounds **11** (2.6 mg, 0.0016%) and **12** (2.2 mg, 0.0014%) were obtained from fraction ACEW 1 by silica gel column chromatography using benzene–CHCl₃ (9:1) as the eluent. Fraction ACEW 8 was rechromatographed on a silica gel column using CHCl₃–Me₂CO (25:1) as the eluent and purified further by preparative TLC (silica gel, *i*-Pr₂O–Me₂CO, 15:1) to obtain compounds **7** (40.0 mg, 0.025%), **4** (2.7 mg, 0.0017%), **5** (2.0 mg, 0.012%), and **6** (2.5 mg, 0.0016%). ACWE 10 was separated on a silica gel column using *i*-Pr₂O–MeOH (6:1) as the eluent to afford four subfractions (ACEW10-1–10-4). Compounds **2** (10.0 mg, 0.0062%), **1** (2.0 mg, 0.0012%), **10** (3.2 mg, 0.002%), **9** (10.2 mg, 0.0063%), and **8** (30.0 mg, 0.0186%) were obtained from subfraction ACEW10-1 using preparative TLC (silica gel, *n*-hexane–Me₂CO, 15:1). Compounds **13** (7.0 mg, 0.0043%), **14** (6.1 mg, 0.0038%), and **15** (3.5 mg, 0.0022%) were isolated from subfraction ACEW10-3 by column chromatography over silica gel using *n*-hexane–EtOAc (1:1) as the eluent. Subfraction

ACEW10-4 was chromatographed on a silica gel column using *n*-hexane–EtOAc (1:1.5) as the eluent to yield compound **3** (3.0 mg, 0.0019%).

The *n*-hexane layer (9.3 g) was chromatographed on silica gel and eluted with EtOAc in *n*-hexane (gradient of 0–100% EtOAc) to obtain 10 fractions. Fraction 4 was chromatographed repeatedly on a silica gel column using *n*-hexane–Me₂CO (19:1) as the eluent to yield **23** (3.0 mg), **24** (6.0 mg, 0.0037%), **25** (4.5 mg, 0.0028%), **38** (3.0 mg, 0.0019%), **34** (22.0 mg, 0.0137%), **35** (90.2 mg, 0.056%), **36** (22.1 mg, 0.0137%), and **37** (16.5 mg, 0.0102%). Compound **37** (41.1 mg, 0.0255%) was also obtained in the same way from fraction 8. The water-insoluble portion (89.5 g) was chromatographed on a silica gel column using CHCl₃–MeOH mixtures of increasing polarity for elution to obtain 10 fractions (WI-1–WI-10). Compounds **16** (2.2 mg, 0.0014%), **20** (2.0 mg, 0.0012%), **21** (14.2 mg,

Figure 6. Selected HMBC correlations of **1** and **4** and NOE correlations of **1**.

0.0088%), **24** (1.0 mg, 0.0006%), **29** (1.29 g, 0.801%), **30** (53.8 mg, 0.0334%), and **36** (62.2 mg, 0.0386%) were obtained from a combined fraction (fractions WI-1 and WI-2) by silica gel column chromatography with gradient elution (CHCl_3 – Me_2CO , 39:1–14:1). Fraction WI-3 was separated on a silica gel column using i - Pr_2O – MeOH (19:1) as the eluent to yield **26** (4.1 g, 2.55%), **33** (11.0 mg, 0.0068%), **31** (122.9 mg, 0.0763%), and **27** (53.0 mg, 0.0329%). Fraction WI-4 was chromatographed on a silica gel column with i - Pr_2O – MeOH (12:1) to give **22** (11.3 mg, 0.007%), **33** (38.0 mg, 0.0236%), **31** (708.0 mg, 0.44%), and **27** (66.5 mg, 0.041%). Fractions WI-5–WI-7 were combined and rechromatographed on a silica gel column with CHCl_3 – MeOH (6:1) as the mobile phase to afford **17** (5.0 mg, 0.0031%), **19** (2.2 mg, 0.0014%), **18** (3.8 mg, 0.0024%), **22** (3.4 mg, 0.00211%), and **28** (2.10 g, 1.3%). Compound **32** (1.16 g, 0.72%) was isolated from a combined fraction (fractions WI-8 and WI-9) by silica gel column chromatography using i - Pr_2O – MeOH (4:1) as the eluent.

3. Results and discussion

The structural elucidation of the five newly isolated benzenoids, benzocamphorins A–E, (**1**–**5**) is described below. Compound **1** was isolated as a pale yellow oil. HRESIMS showed an $[\text{M}+\text{Na}]^+$ ion peak at m/z 285.0740, consistent with the molecular formula $\text{C}_{14}\text{H}_{14}\text{O}_5\text{Na}$. The IR spectrum suggested that **1** was a benzenoid (ν_{max} 1610, 1475, and 1446 cm^{-1}) bearing a conjugated carbonyl (ν_{max} 1663 cm^{-1}). The latter was identified as a methyl ketone based on the carbon resonances at δ 33.2 (CH_3) and 184.8 (qC) as well as the proton resonance at δ 2.45 (3H, s).⁶ The ^1H NMR spectra of **1** showed signals for one methylenedioxy [δ_{H} 5.98 (2H, s)], one aromatic methyl [δ_{H} 2.31 (3H, s)], and two methoxy [δ_{H} 3.88 (3H, s) and 4.02 (3H, s)] groups. In addition, a 1,2-disubstituted alkyne [δ_{C} 87.6 (qC) and 96.0 (qC)] was also observed in the ^{13}C NMR spectrum of **1**. The above characteristic NMR signals were similar to those of the known benzenoid antrocamphin B (**10**), isolated from the same organism.⁶ Detailed inspection of the HMBC spectrum of **1** led to the assignment of a 3-oxobut-1-ynyl group (Fig. 2). The NOE correlations between Me-4 and OMe-5 and between Me-3' and the methylenedioxy protons helped to establish the structure of **1** (Fig. 6).

The molecular formula of **2**, $\text{C}_{15}\text{H}_{16}\text{O}_4$, was established from HRESIMS and ^{13}C NMR spectroscopic data. The IR spectrum showed absorption bands attributable to a benzenoid at ν_{max} 1611, 1473, and 1449 cm^{-1} . The ^1H NMR spectrum of **2** was similar to that of **1**, except that the 3-oxobut-1-ynyl group in **1** was replaced by a 3-methylbut-3-en-1-ynyl group in **2**. This assignment was enforced by the presence of the proton resonances for a 1,1-disubstituted double bond at δ 5.36 (1H, s) and 5.25 (1H, s), which correlated to C-2', C-3', and C-4' in the HMBC spectrum of **2**. In the NOESY spectrum of **2**, a NOE correlation between the methylenedioxy proton and

the Me-3' protons suggested that the methylenedioxy group was located at C-1 and C-2. In addition, the Me-4 protons showed NOE correlations with one proton of the sp^2 methylene group at δ 5.36 and with the OMe-5 protons at δ 3.85, which suggested that Me-4 was adjacent to C-3 and C-5. The locations of all functionalities borne by the benzene ring were thus determined.

The molecular formula of **3** was deduced as $\text{C}_{11}\text{H}_{12}\text{O}_6$ based on the pseudomolecular ion peak at m/z 263.0534 $[\text{M}+\text{Na}]^+$ obtained from HRESIMS. The ^{13}C NMR spectrum of **3** displayed 11 signals including a methyl ester [δ_{C} 164.9 ($\text{C}=\text{O}$) and 52.0 (OMe)], two methoxy [δ_{C} 60.2 (OMe-4) and 56.7 (OMe-5)], a methylenedioxy group [δ_{C} 102.1], an aromatic methine [δ_{C} 104.3 (C-6)], a quaternary carbon [δ_{C} 104.8 (C-1)], and four oxygenated aromatic [δ_{C} 137.5 (C-3), 137.7 (C-4), 144.8 (C-2), and 146.4 (C-5)] carbons. The ^1H NMR spectrum showed a single aromatic proton resonance [δ_{H} 6.90 (s, H-6)], which indicated a pentasubstituted benzene ring in **3**. The above characteristic NMR signals were similar to those of the known compound, methyl 2,5-dimethoxy-3,4-methylenedioxybenzoate (**6**),⁷ suggesting an isomeric relationship between both compounds. The aromatic methine proton showed an HMBC correlation with the carbonyl carbon of the methyl ester and an NOE correlation with the methoxy protons at C-5, suggesting that this proton (H-6) was located between C-1 and C-5. Considering the above evidence coupled with a comparison of the NMR spectroscopic data of **3** with those of **6**, the structure of **3** was thus determined as methyl 4,5-dimethoxy-2,3-methylenedioxybenzoate.

Compound **4** was isolated as a white powder and exhibited a $[\text{M}+\text{Na}]^+$ peak at m/z 399.1051, corresponding to the molecular formula of $\text{C}_{19}\text{H}_{20}\text{O}_8\text{Na}$ and 10° of unsaturation. Its IR spectrum showed absorption bands at 1619, 1497, 1489, 1448, and 1427 cm^{-1} , disclosing that **4** is a benzenoid. Its ^1H NMR spectrum, coupled with a HMQC experiment, showed signals for two methylenedioxy groups at δ 5.98 and 5.94, three methoxy groups at δ 3.93, 3.88, and 3.82, and two aromatic methyl groups at δ 2.06 and 2.03. One remaining aromatic methine and eleven aromatic quaternary carbons were also observed in the ^{13}C NMR spectrum of **4**. Thus, **4** might be a benzoic dimer. In subunit A, the HMBC correlations from the methyl proton at δ_{H} 2.06 to the carbons at C-1', C-2', and C-6', from the methylenedioxy protons at δ_{H} 5.98 to the carbons at C-3' and C-4', and from the phenyl proton at δ_{H} 5.92 (H-6') to the carbons at C-1', C-2', C-4', and C-5' (Fig. 2) in combination with selective 1D NOESY experiments (Me-1'/OMe-2', Me-1'/H-6', and OMe-2'/methylenedioxy protons at δ_{H} 5.85) (Fig. 7) enforced the locations of all functional groups on the benzene ring.

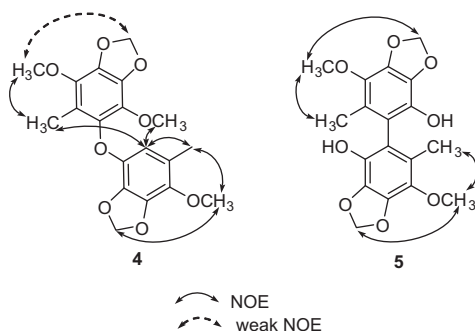


Figure 7. NOE correlations of **4** and **5**.

Table 1

Cytotoxic activity of **7**–**9**, **13** and **14**, **20** and **21**, **25**–**33**, and **36**

Compound	Cell lines ED ₅₀ (μg/mL)			
	Daoy	Hep2	MCF-7	Hela
7	—	—	—	—
8	—	—	—	—
9	5.9	10.5	3.4	6.9
13	—	—	—	—
14	—	—	—	—
20	5.2	7.0	6.6	9.0
21	4.4	3.0	7.9	8.9
25	— ^a	—	8.7	11.3
26	—	16.6	—	—
27	—	—	—	—
28	—	—	—	—
29	—	—	—	—
30	13.2	—	13.3	—
31	—	—	—	—
32	—	—	—	—
33	—	—	—	—
36	—	—	—	—
Mitomycin C	0.1	0.1	0.1	0.2

^a ED₅₀ > 20 μg/mL.

Table 2Effects of **2**, **7–9**, **17**, **21**, and **24–37** on NOX activity^a in BV2 murine microglial cells and PMNs and NOS activity^b in murine microglial cells

Compound	IC ₅₀ (μM) in NOX		IC ₅₀ (μM) in NOS
	Activity from BV2 cell lysate	fMLP-induced NOX activation in PMN	
2	ND	14.4 ± 4.9 [*]	12.1 ± 0 [*]
7	ND	15.5 ± 3.3 [*]	16.2 ± 1.4 [*]
8	ND	19.9 ± 3.0 [*]	29.1 ± 4.4 [*]
9	50.1 ± 3.3 [*]	15.1 ± 4.1 [*]	7.2 ± 1.0 [*]
17	ND	32.1 ± 3.5 [*]	15.7 ± 0.9 [*]
21	ND	11.2 ± 2.3 [*]	2.5 ± 0.6 [*]
24	ND	17.5 ± 3.9 [*]	12.7 ± 2.2 [*]
25	ND	15.8 ± 4.0 [*]	1.6 ± 0.6 [*]
26	ND	22.1 ± 6.7 [*]	3.6 ± 0.8 [*]
27	ND	ND	9.6 ± 0.7 [*]
28	40.3 ± 3.5 [*]	ND	16.2 ± 0.9 [*]
29	ND	8.4 ± 2.1 [*]	0.6 ± 0.3 [*]
30	45.9 ± 7.9 [*]	29.2 ± 6.7 [*]	4.1 ± 0.5 [*]
31	ND	22.6 ± 3.3 [*]	4.2 ± 1.2 [*]
32	ND	47.2 ± 8.4 [*]	ND
33	16.0 ± 8.1 [*]	18.1 ± 5.9 [*]	2.5 ± 0.3 [*]
34	ND	21.9 ± 6.3 [*]	22.3 ± 2.9 [*]
35	ND	27.9 ± 5.6 [*]	30.6 ± 0.8 [*]
36	ND	16.2 ± 4.3 [*]	1.5 ± 0.7 [*]
37	ND	20.3 ± 6.4 [*]	6.3 ± 1.8 [*]
DPI	0.4 ± 0.2	0.3 ± 0.1	—
L-NAME	—	—	25.8 ± 2.5

ND, values not detectable; ‘—’, samples not tested.

^a NOX activity was measured as ROS production by triggering with NADPH (200 μM) or fMLP (2 μM) in the presence of test drugs (1–50 μM) in BV2 cell lysate or PMN. DPI (a NOX inhibitor) was included as a positive control for NOX inhibition.^b NO production was measured in the presence of test drugs (1–50 μM). L-NAME (a non-selective NOS inhibitor) was included as a positive control. Data were calculated as 50% inhibitory concentration (IC₅₀) and expressed as the mean ± SEM from three to six experiments performed on different days using BV2 cell lysate or PMN from different passages or donors.^{*} *P* < 0.05 as compared with relative positive control, respectively.

The carbons in subunit B were deduced as a benzenoid containing a methyl, one methylenedioxy, and two methoxy substituents. The HMBC correlations from Me-1 protons to C-2 and C-6 carbons as well as the selective 1D NOESY enhancements of Me-1/OMe-2, H-6'/Me-1, and H-6'/OMe-5 established the structure of subunit B. Based on the carbon resonances of C-6 and C-5' at 139.5 and 137.25, respectively, the two subunits were connected by an oxygen atom, which also was consistent with the molecular formula of **4**.

The HRESIMS spectrum of **5** disclosed that it possesses a molecular ion peak at *m/z* 385.0897, corresponding to the molecular formula C₁₈H₁₈O₈Na. The IR absorption bands at ν_{max} 3526, 1512, and 1460 cm^{−1} suggested that **5** was a phenolic derivative. The appearance of only nine signals in the ¹³C NMR spectrum revealed that the compound is symmetric and homodimeric. Analysis of the ¹H and ¹³C NMR spectra of **5** suggested that half of the molecular possesses methoxy [δ_H 3.93 (s); δ_C 60.1(CH₃)], methylenedioxy [δ_H 6.02 (s); δ_C 101.8 (CH₂)], and aromatic methyl [δ_H 1.85 (s); δ_C 12.6 (CH₃)] groups, as well as four oxygenated aromatic carbons [δ_C 139.1 (qC), 136.4 (qC), 133.6 (qC), and 133.3 (qC)] and two quaternary carbons [δ_C 123.8 (qC) and δ_C 114.5 (qC)]. The aromatic methyl protons showed HMBC correlations to C-1, C-2, and C-6, suggesting that this methyl group was positioned between C-2 and C-6, to which the other molecular half was attached. In the NOESY spectrum of **5** (Fig. 7), the methylenedioxy protons showed an NOE correlation with the OMe-2 carbon, suggesting that this substituent was positioned at C-3 and C-4. Thus, the one remaining hydroxy group should be positioned at C-5. The structure of **5** was unambiguously determined as shown in Figure 1.

The structural characterization of 10 newly isolated triterpenoids, camphoratin A–J (**16–25**), was reported previously in Ref. 13. In addition, 23 known compounds were identified by the

comparison of their physical and spectroscopic data with those of corresponding authentic samples, including seven benzenoids [2,5-dimethoxy-3,4-methylenedioxybenzoate (**6**)⁷, 2,2',5,5'-tetramethoxy-3,4,3',4'-bi-methylenedioxy-6,6'-dimethylbiphenyl (**7**)⁸, 4,7-dimethoxy-5-methyl-1,3-benzodioxole (**8**)⁸, antrocamphins A and B (**9** and **10**)⁶, syringic acid (**11**)⁹ and 3,4,5-trimethoxybenzoic acid (**12**)¹⁰, three lignans [4-hydroxysesamin (**13**)¹¹, (+) sesamin (**14**)¹¹ and aptosimon (**15**)¹², and 13 triterpenoids [zhankuic acids A–C (**26–28**)^{14,15}, zhankuic acid A methyl ester (**29**)¹⁴, antcin A (**30**)¹⁵, antcin C (**31**)¹⁵, antcin K (**32**)¹⁶, methyl antcin H (**33**)¹⁷, eburicol (**34**)¹⁸, ergosterol D (**35**)¹⁹, methyl 4α-methylergost-8,24 (28)-dien-3,11-dion-26-oate (**36**)²⁰, ergosterol peroxide (**37**)²¹, and ergosta-2,4,8(14),22-tetraen-3-one (**38**)²².

Compounds **7–9**, **13**, **14**, **20**, **21**, **25–33**, and **36** were first assayed for cytotoxic activity against Doay (human medulloblastoma), Hep2 (human laryngeal carcinoma), MCF-7 (human breast adenocarcinoma), and Hela (human cervical epitheloid carcinoma) cell lines. Compounds **9** and **21** showed moderate cytotoxicity against MCF-7 and Hep2 cell lines with ED₅₀ values of 3.4 and 3.0 μg/mL, respectively (Table 1). The other tested compounds showed marginal or little cytotoxicity (threshold for activity is considered 4 μg/mL) against the above cancer cell lines.

The anti-inflammatory effects of **2**, **7–9**, **17**, **21**, and **24–37** were then evaluated by examining their effects on lipopolysaccharide (LPS)-induced iNOS-dependent NO production and NADPH oxidase (NOX)-dependent reactive oxygen species (ROS) production in BV2 murine microglial cells and polymorphonuclear neutrophils (PMNs) (Table 2). Triterpenoids **21**, **25**, **26**, **29–31**, **33**, and **36** inhibited NOS activity significantly with IC₅₀ values of 2.5, 1.6, 3.6, 0.6, 4.1, 4.2, 2.5, and 1.5 μM, respectively. They were more potent than *N*-nitro-L-arginine methyl ester (L-NAME) (IC₅₀: 25.8 μM), a non-specific NOS inhibitor, at inhibiting LPS-induced NO production. Except for **8** and **35**, the remaining tested compounds also effectively inhibited NOS activity with IC₅₀ values ranging from 6.3 to 22.3 μM. NOX is the major ROS-producing enzyme in activated inflammatory cells.²³ We previously reported that drugs with anti-inflammatory activity also show potent NOX-inhibitory action.^{24,25} Therefore, we evaluated the isolates for effects on NOX activity in lysates of microglial cells and PMNs. Our data suggest that none of the tested compounds were potent inhibitors of NOX, relative to the specific NOX inhibitor diphenyleneiodonium (DPI) (IC₅₀ 0.4 and 0.3 μM in lysates of microglial cells and PMNs, respectively) (Table 2).

Based on an overview of the biological data, the following structure-activity relationship (SAR) conclusions were noted regarding the NOS inhibitory activity for compounds **17**, **21**, and **24–37** (Table 2). Among the tested compounds, the 3-ketone triterpenoids were more active than the corresponding 3-hydroxy analogues (e.g., **21** vs **17**; **27** vs **16**). Similarly, introduction of a hydroxy group to C-4 resulted in a dramatic loss of activity (e.g., **27** vs **32**). It is apparent that a less polar A ring contributed to increased activity. In addition, comparison of triterpenoids with different substituents at C-7 revealed that the rank order of potency was 7-ketone (**29**) > 7-methylene (**30**) ≈ 7-hydroxy (**31**). On the other hand, compound **25**, the rare example with a 14β-hydrogen configuration, was less potent than the normal triterpene (**29**, 14α-hydrogen). A comparison of the carboxylic acids and methyl carboxylates revealed that the latter were slightly more potent than the former (e.g., **21** vs **31**; **29** vs **26**). Consequently, the most active **29** could be reasonably explained by the fact that it possesses 7-ketone, less polar A ring, and methyl carboxylate functionalities.

In conclusion, the results from the anti-inflammatory assays revealed that the triterpenoids **21**, **25**, **26**, **29–31**, **33**, and **36** have potent NO-reducing activity in microglial cells. Thus, triterpenoids rather than benzenoids might be the active components of the folk remedy using *T. camphoratus* for the treatment of some

inflammatory related disorders. However, continued investigation of related triterpenoids coupled with structure modification studies could be helpful to develop and optimize lead chemotherapeutic agents.

4. Experimental

4.1. General experimental procedures

Melting points were determined on a Yanagimoto MP-S3 micro-melting point apparatus. IR spectra were recorded on a Shimadzu FTIR spectrometer Prestige-21. Optical rotations were measured using a Jasco DIP-370 polarimeter. UV spectra were obtained on a Hitachi UV-3210 spectrophotometer. ESI and HRESI mass spectra were recorded on a Bruker APEX II mass spectrometer. The NMR spectra, including ^1H NMR, ^{13}C NMR, COSY, NOESY, HMBC, HMQC experiments, were recorded on Bruker AVANCE-500 and AMX-400. Silica gel (E. Merck 70–230, 230–400 mesh) was used for column chromatography.

4.1.1. Benzocamphorin A (1)

Pale yellow oil; UV (MeOH) λ_{max} (log ϵ) 214 (3.44), 275 (2.63), 315 (2.94) nm; IR (KBr) ν_{max} 2925, 2854, 1663, 1610, 1475, 1446, 1381, 1277, 1212, 1054 cm^{-1} ; ^1H NMR (CDCl_3 400 MHz) δ_{H} 5.98 (2H, s, OCH_2O), 4.02 (3H, s, OMe-6), 3.88 (3H, s, OMe-5), 2.45 (3H, s, 4'), 2.31 (3H, s, Me-4); ^{13}C NMR (CDCl_3 , 100 MHz) δ_{C} 184.8 (C-3'), 142.5 (C-2), 142.0 (C-6), 137.5 (C-5), 136.2 (C-1), 131.3 (C-4), 106.6 (C-3), 102.2 (OCH_2O), 96.0 (C-2'), 87.6 (C-1'), 60.7 (OMe-6), 60.5 (OMe-6), 33.2 (C-4'), 14.4 (Me-4); ESIMS m/z 285 $[\text{M}+\text{Na}]^+$; HRESIMS m/z 285.0740 (calcd for $\text{C}_{14}\text{H}_{14}\text{O}_5\text{Na}$, 285.0739).

4.1.2. Benzocamphorin B (2)

Pale yellow oil; UV (MeOH) λ_{max} (log ϵ) 215 (4.38), 254 (3.78), 287 (4.04) nm; IR (KBr) ν_{max} 2943, 2781, 1611, 1473, 1449, 1389, 1274, 1207, 1050 cm^{-1} ; ^1H NMR (CDCl_3 , 400 MHz) δ_{H} 5.36 (1H, br s, H-5'b), 5.26 (1H, br s, H-5'a), 5.92 (2H, s, OCH_2O), 3.97 (3H, s, OMe-6), 3.85 (3H, s, OMe-5), 2.26 (3H, s, Me-4), 2.00 (3H, s, Me-3'); ^{13}C NMR (CDCl_3 , 100 MHz) δ_{C} 139.8 (C-6), 139.4 (C-1), 137.1 (C-5), 136.2 (C-2), 127.8 (C-4), 127.2 (C-3'), 120.9 (C-5'), 109.8 (C-3), 101.4 (OCH_2O), 97.5 (C-2'), 83.5 (C-1'), 60.3 (OMe-6), 59.9 (OMe-5), 23.5 (Me-4), 13.8 (Me-3'); ESIMS m/z 283 $[\text{M}+\text{Na}]^+$; HRESIMS m/z 283.0944 (calcd for $\text{C}_{15}\text{H}_{16}\text{O}_4\text{Na}$, 283.0946).

4.1.3. Benzocamphorin C (3)

Colorless oil; UV (MeOH) λ_{max} (log ϵ) 220 (3.69), 263 (3.36), 320 (2.95) nm; IR (KBr) ν_{max} 2920, 2851, 1699, 1629, 1503, 1437, 1201, 1097 cm^{-1} ; ^1H NMR (CDCl_3 , 300 MHz) δ_{H} 6.90 (1H, s, H-6), 6.04 (2H, s, OCH_2O), 4.10 (3H, s, OMe-4), 3.89 (3H, s, COOCH_3), 3.85 (3H, s, OMe-5); ^{13}C NMR (CDCl_3 , 75 MHz) δ_{C} 164.9 (COOCH_3), 146.4 (C-5), 144.8 (C-2), 137.7 (C-4), 137.5 (C-3) 104.8 (C-1), 104.3 (C-6), 102.1 (OCH_2O), 60.2 (OMe-4), 56.7 (OMe-5), 52.0 (COOCH_3); ESIMS m/z 263 $[\text{M}+\text{Na}]^+$; HRESIMS m/z 263.0534 (calcd for $\text{C}_{11}\text{H}_{12}\text{O}_6\text{Na}$, 263.0532).

4.1.4. Benzocamphorin D (4)

White powder; mp 73–74 $^{\circ}\text{C}$; UV (MeOH) λ_{max} (log ϵ) 207 (4.80), 279 (3.39) nm; IR (KBr) ν_{max} 2939, 2892, 1619, 1497, 1448, 1427, 1254, 1232, 1119, 1085, 1057, 1024, 956 cm^{-1} ; ^1H NMR (CDCl_3 500 MHz) δ_{H} 2.03 (3H, s, CH_3 -1), 2.06 (3H, s, CH_3 -1'), 3.82 (3H, s, OCH_3 -5), 3.88 (3H, s, OCH_3 -2'), 3.93 (3H, s, OCH_3 -2), 5.92 (1H, s, H-6'), 5.94 (2H, s, OCH_2O -3, 4), 5.98 (2H, s, OCH_2O -3, 4'); ^{13}C NMR (CDCl_3 , 125 MHz) δ_{C} 9.3 (CH_3 -1), 15.8 (CH_3 -1'), 59.8 (OCH_3 -2'), 60.0 (OCH_3 -2), 60.6 (OCH_3 -5), 101.4 (OCH_2O -3, 4), 101.6 (OCH_2O -3', 4'), 109.5 (C-6'), 117.6 (C-1), 123.6 (C-1'), 133.0

(C-5), 134.3 (C-3'), 135.6 (C-4), 136.7 (C-2'), 136.8 (C-2), 137.25 (C-5'), 137.29 (C-3), 138.7 (C-4'), 139.5 (C-6); ESIMS m/z 399 $[\text{M}+\text{Na}]^+$; HRESIMS m/z 399.1052 (calcd for $\text{C}_{19}\text{H}_{20}\text{O}_8\text{Na}$, 399.1056).

4.1.5. Benzocamphorin E (5)

Colorless oil; UV (MeOH) λ_{max} (log ϵ) 208 (4.91), 283 (3.80) nm; IR (KBr) ν_{max} 3526, 2928, 2859, 1713, 1492, 1460, 1261, 1035 cm^{-1} ; ^1H NMR (CDCl_3 , 500 MHz) δ_{H} 1.85 (6H, s, CH_3 -1, 1'), 3.93 (6H, s, OCH_3 -2, 2'), 6.02 (4H, s, OCH_2O -3, 4; 3', 4'); ^{13}C NMR (CDCl_3 , 125 MHz) δ_{C} 12.6 (CH_3 -1, 1'), 60.1 (OCH_3 -2, 2'), 101.8 (OCH_2O -3, 4; 3', 4'), 114.5 (C-6, 6'), 123.8 (C-1, 1'), 133.3 (C-5, 5'), 133.6 (C-4, 4' or C-3, C-3'), 136.4 (C-2, 2'), 139.1 (C-4, 4' or C-3, C-3'); ESIMS m/z 385 $[\text{M}+\text{Na}]^+$; HRESIMS m/z 385.0897 (calcd for $\text{C}_{18}\text{H}_{18}\text{O}_8\text{Na}$, 385.0899).

4.2. Cytotoxicity assay

Cytotoxicity was tested against Doay, Hep2, MCF-7, and Hela cell lines, using a MTT colorimetric assay method. The assay procedure was carried out as previously described,²⁶ and mitomycin was used as positive control.

4.3. Microglial cell culture and measurements of NO

The BV2 murine microglial cell line was cultured and production of NO was measured by the methods as described in our prior report.²⁷ L-NAME (a non-selective NOS inhibitor) was included as a positive control.

4.4. Measurement of NOX activity

NOX activity was measured as described previously.²⁷ DPI (a NOX inhibitor) was included as a positive control.

Acknowledgments

The authors acknowledge the financial support from the National Science Council, Taiwan, Republic of China and Dr. Tun-Tschu Chang (Division of Forest Protection, Taiwan Forestry Research Institute, Taipei, Taiwan) for his identification of *T. camphoratus*. Thanks are also due to the partial support from NIH grant CA-17625 awarded to K.-H.L.

References

- Wu, S. H.; Yu, Z. H.; Dai, Y. C.; Chen, C. T.; Su, C. H.; Chen, L. C.; Hsu, W. C.; Hwang, G. Y. *Fung. Sci.* **2004**, *19*, 109.
- Tsai, Z. T.; Liaw, S. L. *The Use and the Effect of Ganoderma*; Sang-Yun Press: Taichung, Taiwan, 1982.
- Chen, C. J.; Su, C. H.; Lan, M. H. *Fung. Sci.* **2001**, *16*, 65.
- Liu, D. Z.; Liang, H. J.; Chen, C. H.; Su, C. H.; Lee, Z. H.; Huang, C. T.; Hou, W. C.; Lin, S. Y.; Zhong, W. B.; Lin, P. J.; Hung, L. F.; Liang, Y. C. *J. Ethnopharmacol.* **2007**, *113*, 45.
- Rao, Y. K.; Fang, S. H.; Tzeng, Y. M. *J. Ethnopharmacol.* **2007**, *114*, 78.
- Chen, J. J.; Lin, W. J.; Liao, C. H.; Shieh, P. C. *J. Nat. Prod.* **2007**, *70*, 989.
- Huang, K. F.; Huang, W. M.; Chiang, H. C. *Chin. Pharm. J.* **2001**, *53*, 327.
- Chiang, H. C.; Wu, D. P.; Cherng, I. W.; Ueng, C. H. *Phytochemistry* **1995**, *39*, 613.
- Herz, W.; Kumar, N. *Phytochemistry* **1981**, *20*, 247.
- Tezuka, Y.; Yoshida, Y.; Kikuchi, T.; Xu, G. *J. Chem. Pharm. Bull.* **1993**, *41*, 1346.
- Wu, D. P.; Chiang, H. C. *J. Chin. Chem. Soc.* **1995**, *42*, 797.
- Brieskorn, C. H.; Huber, H. *Tetrahedron Lett.* **1976**, 2221.
- Wu, S. J.; Leu, Y. L.; Chen, C. H.; Chao, C. H.; Shen, D. Y.; Chan, H. H.; Lee, E. J.; Wu, T. S.; Wang, Y. H.; Shen, Y. C.; Lee, K. H. *J. Nat. Prod.* **2010**, doi:10.1021/np1002143.
- Chen, C. H.; Yang, S. W.; Shen, Y. C. *J. Nat. Prod.* **1995**, *58*, 1655.
- Cherng, I. H.; Chiang, H. C.; Cheng, M. C.; Wang, Y. J. *Nat. Prod.* **1995**, *58*, 365.
- Shen, C. C.; Kuo, Y. C.; Huang, R. L.; Lin, L. C.; Don, M. J.; Chang, T. T.; Chou, C. J. *J. Chin. Med.* **2003**, *14*, 247.
- Cherng, I. W.; Wu, D. P.; Chiang, H. C. *Phytochemistry* **1996**, *41*, 263.
- Shirane, N.; Takenaka, H.; Ueda, K.; Hashimoto, Y.; Katoh, K.; Ishii, H. *Phytochemistry* **1996**, *41*, 1301.
- Abraham, R. J.; Monasterios, J. R. *J. Chem. Soc., Perkin Trans. II* **1974**, 662.

20. Wu, D. P.; Chiang, H. C. *J. Chin. Chem. Soc.* **1995**, 42, 797.
21. Rösecke, J.; König, W. A. *Phytochemistry* **2000**, 54, 757.
22. Quang, D. N.; Bach, D. D. *Nat. Prod. Res.* **2008**, 22, 901.
23. Van den Worm, E.; Beukelman, C. J.; Van den Berg, A. J.; Kroes, B. H.; Labadie, R. P.; Van Dijk, H. *Eur. J. Pharmacol.* **2001**, 433, 225.
24. Lin, L. C.; Wang, Y. H.; Hou, Y. C.; Chang, S.; Liou, K. T.; Chou, Y. C.; Wang, W. Y.; Shen, Y. C. *J. Pharm. Pharmacol.* **2006**, 58, 129.
25. Liou, K. T.; Shen, Y. C.; Chen, C. F.; Tsao, C. M.; Tsai, S. K. *Eur. J. Pharmacol.* **2003**, 475, 19.
26. Shen, Y. C.; Wang, S. S.; Pan, Y. L.; Lo, K. L.; Chakraborty, R.; Chien, C. T.; Kuo, Y. H.; Lin, Y. C. *J. Nat. Prod.* **2002**, 65, 1848.
27. Wang, Y. H.; Wang, W. Y.; Chang, C. C.; Liou, K. T.; Sung, Y. J.; Liao, J. F.; Chen, C. F.; Chang, S.; Hou, Y. C.; Chou, Y. C.; Shen, Y. C. *J. Biomed. Sci.* **2006**, 13, 127.